Proceedings of the 41st Polish Seminar on Positron Annihilation, Lublin, September 9–13, 2013

Defects in Zirconia Nanomaterials Doped with Rare-Earth Oxides

I. Prochazka[a,*], J. Cizek[a], O. Melikhova[a], T.E. Konstantinova[b] and I.A. Danilenko[b]

[a]Charles University in Prague, Faculty of Mathematics and Physics, Department of Low Temperature Physics V Holesovickach 2, CZ-180 00 Praha 8, Czech Republic

[b]National Academy of Sciences of Ukraine, Donetsk Institute for Physics and Engineering named after O.O. Galkin Luxemburg Str. 72, 83114 Donetsk, Ukraine

Positron lifetime and coincidence Doppler broadening measurements on ZrO_2+3 mol.% RE_2O_3 (RE = Eu, Gd, Lu) nanopowders and ceramics obtained by sintering these nanopowders are reported. The initial nanopowders were prepared by a co-precipitation technique and exhibited a mean particle size of $\approx$ 15 nm. The nanopowders were calcined and pressure-compacted. All compacted nanopowders exhibited the prevailing tetragonal phase with at most 15% of the monoclinic admixture. Positrons in compacted nanopowders were found to annihilate almost exclusively at grain boundaries: (i) vacancy-like misfit defects along grain boundaries and (ii) larger defects situated at intersections of grain boundaries (triple points). In nanopowders, a small portion of positrons formed positronium in pores between crystallites. Sintering of nanopowders at 1500 °C caused a substantial grain growth and formation of ceramics. Sintering-induced grain growth led to a disappearance of the triple points and pores. The ceramics containing Eu and Gd dopants consist of mixture of the monoclinic and the tetragonal phase, while the ceramics with Lu dopant exhibits almost exclusively the tetragonal phase.

DOI: 10.12693/APhysPolA.125.760

PACS: 81.07.Wx, 61.46.Hk, 78.70.Bj

1. Introduction

Zirconium dioxide (zirconia) exhibits advantageous mechanical, thermal, electronic and other properties [1]. This is why zirconia is widely used in many areas of practice, in particular, in the ceramic industry. However, a stabilisation of the high-temperature tetragonal (t-) and cubic (c-) zirconia phases is necessary to avoid a mechanical deterioration of this material when repeated phase transitions to/from the room temperature monoclinic (m-) zirconia occur. A phase stabilisation of zirconia can be accomplished by doping zirconia with a proper metal oxide giving rise to a formation of a solid solution of the dopant in the zirconia lattice. A traditional zirconia phase stabiliser, nowadays, is the trivalent yttrium oxide (yttria) [1]. The Y^{3+} ionic radius exceeding considerably that of Zr^{4+} (0.9 and 0.7 Å, respectively) likely assists to yttria stabilisation ability. Since yttria is a relatively expensive substance, a searching for other metal oxides which might induce a phase stabilisation of zirconia is of a great interest. Among the likely candidates for zirconia phase stabilisers, the rare-earth (RE) oxides may be considered because of some chemical properties of RE elements and their ionic radii ($\approx$ 0.9 to 1.0 Å) are similar to yttrium.

Characteristics of functional ceramic materials may be improved if the ceramic is manufactured by sintering nanoscopic particles of $\approx$ 10 nm size [2]. In such a case, grain boundaries (GBs) and defects associated to GBs become to play an enhanced role and influence microstructure evolution during sintering.

Indeed, reaching of phase stability is not the only benefit of zirconia doping with other metal cations. Such a doping may also take a positive effect on e.g. mechanical properties, ionic conductivity, desired sintering temperature, and thermal stability of the material [3]. When the impurity metal valence is lower than that of Zr (4+), stoichiometry violation generates a huge amount of oxygen vacancies and related defects complexes.

The present study was focused on the characterisation of defects in zirconia doped with trivalent RE oxides (RE = Eu, Gd and Lu). Pressure-compacted nanopowders and ceramics made by sintering of these nanopowders were investigated using positron lifetime (PL) and coincidence Doppler broadening (CDB) spectroscopies. The study represents an extension of our recent research on yttria-stabilised zirconia (YSZ) nanomaterials reviewed in [4]. To authors' knowledge, no positron annihilation studies of the zirconia nanosystems doped with RE_2O_3 were reported before in the published literature.

2. Experimental part

2.1. Zirconia + RE_2O_3 samples

Particular systems investigated in the present work were ZrO_2 + 3 mol.% Eu_2O_3, ZrO_2 + 3 mol.% Gd_2O_3 and ZrO_2 + 3 mol.% Lu_2O_3 solid solutions. They are denoted below as Z3E, Z3G and Z3L, respectively. The initial nanopowders were prepared by the co-precipitation technique similar to that described in [2, 5], taking water

*corresponding author; e-mail: ivan.prochazka@mff.cuni.cz

solutions of desired salts in stoichiometric proportions. The resulting nanopowders were then calcined at 700 °C for 2 h in air. Finally, the calcined nanopowders were compacted under a uniaxial pressure of 200 MPa so that the disk-shaped pellets were formed (≈ 10 mm in diameter and 2 mm in thickness). To produce ceramic specimens, the pellets were subject to sintering at 1500 °C for 1 h in air with subsequent slow cooling down to room temperature. The mean nanoparticle sizes, d, and the phase compositions of the samples studied were characterised using XRD. Basic characteristics of the studied materials were summarised in Table I.

Basic characteristics of specimens studied in the present work. TABLE I

Sample abbrev.	Composition	Status	Phase composition[a]	d [nm]
Z3Ep		nanopowder	t98.5% + m1.5%	17.2
	ZrO_2+3 mol.% Eu_2O_3			
Z3Ec		ceramics	t46% + m54%	
Z3Gp		nanopowder	t95% + m5%	17.8
	ZrO_2+3 mol.% Gd_2O_3			
Z3Gc		ceramics	t27.5% + m72.5%	
Z3Lp		nanopowder	t87% + m13%	18.7
	ZrO_2+3 mol.% Lu_2O_3			
Z3Lc		ceramics	t98.5% + m1.5%	

[a] t — tetragonal phase, m — monoclinic phase

2.2. Apparatus and data taking

Positron sources utilised in PL and CDB measurements were made as a small drop of ^{22}Na carbonate in water solution (iThemba LABS) deposited and dried between the 2 μm thick Mylar ® C (DuPont) covering foils. The activity of sources amounted typically 1 MBq.

The PL measurements were carried out using a digital spectrometer described in [6]. The spectrometer was equipped with BaF_2 scintillators and Hamamatsu H3378 photomultipliers and exhibited a time resolution of 145 ps (the FWHM of resolution function for ^{22}Na). Typically, 10^7 coincidence events were accumulated in each PL spectrum. The PL spectra were decomposed into the discrete components by means of a procedure [7] based on the maximum-likelihood principle. A contribution of positron annihilations in the source salt and covering foils was determined using a well-annealed high-purity α-iron specimen and recalculated to zirconia according to the method given in [8].

The CDB measurements were performed using a coincidence spectrometer [9] equipped with two HPGe detectors and fast 12-bit digitisers. The spectrometer exhibited an energy resolution of 0.9 keV and a peak-to-background ratio better than 10^5. At least 10^8 coincidence events were collected in each 2D energy spectra. The Doppler-broadened profiles (DBPs) were cut from these spectra. The CDB results were then displayed as the ratios of the DBPs to the DBP measured for a well-annealed coarse-grained pure Zr (99.9%) reference specimen.

Both the PL and CDB measurements were conducted in air at ambient temperature.

3. Results and discussion

The lifetimes and the relative intensities of discrete components resolved in measured PL spectra were summarised in Table II. The longest lifetime components of Table, $\tau_4 \approx 15$ ns and a weak relative intensity I_4, inevitably indicate *ortho*-positronium (o-Ps) formation in the Z3E, Z3G, and Z3L compacted nanopowders. Corresponding *para*-positronium (p-Ps) component was always subtracted in PL spectra decompositions as a fixed component (not shown in Table II, lifetime $\tau_{\mathrm{pPs}} = 125$ ps, intensity $I_{\mathrm{pPs}} = I_4/3$) and reflected in the normalisation of the intensities shown in Table II ($I_1 + I_2 + I_3 + 4I_4/3 = 100\%$).

TABLE II

Positron lifetimes, τ_i, and relative intensities, I_i (i = 1, 2, 3, 4), resolved in the present study. The standard deviations are shown in parentheses in the units of the last significant digit.

Sample	τ_1 [ps]	I_1 [%]	τ_2 [ps]	I_2 [%]	τ_3 [ps]	I_3 [%]	τ_4 [ns]	I_4 [%]
Z3Ep			213(2)	40.4(7)	421(2)	54.6(7)	15.7(2)	3.7(5)
Z3Ec	154(5)	36(6)	219(4)	64(6)				
Z3Gp			253.2(7)	62.6(4)	499(3)	28.1(3)	14.7(1)	6.9(3)
Z3Gc	142(5)	24(3)	219(2)	76(3)				
Z3Lp			213(2)	46.9(9)	435(3)	45.5(9)	16.5(1)	5.7(4)
Z3Lc	163(5)	59(12)	203(6)	41(12)				

Positronium formation found in Z3E, Z3G, and Z3L compacted nanopowders should be regarded as a strong evidence of porosity in these materials. Using the semiempirical formula [10, 11], the pore sizes (diameters) were estimated from o-Ps lifetimes $\tau_4 \approx 15$ ns of Table II as ≈ 1.8 nm. These results are similar to findings obtained previously for YSZ [12] and ceria-stabilised zirconia (CeSZ) [13] nanopowders of a comparable particle sizes (10 to 20 nm diameter) prepared by the co-precipitation technique. Based on simple geometrical considerations [14], it is thus simultaneously suggested that the main contribution to the o-Ps components observed in compacted nanopowders comes from Ps formation in the cavities between primary nanoparticles.

Positrons which did not form Ps in compacted nanopowders give rise to two components of PL spectra with lifetimes τ_2 ranging from ≈ 200 to 250 ps and τ_3 lying between 400 and 500 ps, see Table II. This situation is again similar to the cases of the YSZ and CeSZ nanopowders [12, 13]. Taking into account that both lifetimes lie well-above the bulk lifetime, $\tau_{\mathrm{b}} \approx 150$ ps, expected in the perfect ZrO_2 lattice [12], we attribute these components to positron trapping in two kinds of defects associated to GBs: (i) the vacancy-like misfit defects situated along GBs and (ii) larger open-volume defects at the intersections of three GBs (triple points). Since typical positron diffusion lengths exceed several times the size of nanograins, positrons thermalised inside grains may easily reach GBs and get trapped in open-volume

defects there. From the same reason, positron trapping in defects in grain interiors plays almost negligible role in compacted nanopowders.

It is seen in Table II that the τ_4- and τ_3-components vanished in PL spectra of all three ceramics. This can be expected and should be ascribed to a substantial grain growth induced by sintering at 1500 °C which resulted in a disappearance of pores and a drastic decrease in the density of triple points so that the fraction of positrons trapped there became negligible. Components with $\tau_2 \approx 210$ ps, i.e. similar to those seen in nanopowders, were found in Z3E, Z3G, and Z3L ceramics. Additional components with a shorter lifetime of $\tau_1 \approx 150$ ps haves appeared in each of the three ceramics, see Table II. In the ceramics, the volume fraction of GBs is drastically decreased compared to the nanopowders and defects inside grains become more important for positrons. Theoretical calculations have proved that zirconium vacancy (V_{Zr}) in the zirconia lattice is an efficient positron trap [12]. Positron trapping with a lifetime of $\tau_V \approx 175$ ps in V_{Zr}-like defects was observed in the YSZ single crystal as well as in the YSZ sintered ceramics [12, 15]. In the YSZ ceramics, moreover, the V_{Zr}-like defects were shown to reside in the grain interiors [15]. We shall therefore assume that the shortest apparent component of lifetime τ_1 in PL spectra of all the three ceramics may be a lifetime doublet composed of the two closely spaced real components. These originated from annihilations of (i) positrons trapped in the V_{Zr}-like defects inside grains, similarly to the case of YSZ ceramics [15], and (ii) positrons in the delocalised state. It seems reasonable to consider the bulk positron lifetime, i.e. the lifetime in the perfect zirconia lattice, to be $\tau_b \approx 150$ ps which is suggested by detailed theoretical calculations [12]. Then the expected two real lifetimes composing this lifetime doublet are ≈ 175 ps and below ≈ 150 ps, respectively. Thus the situation in ceramics has become reversed with respect to the case of nanopowders as far as the positron trapping mechanism is concerned: as grains grow due to sintering, the chance of positrons to reach GBs becomes much lower and positron trapping in defects inside grains (V_{Zr}-like defects) starts to be the prevailing trapping mechanism. One should also note that V_{Zr}-type defects are not created during sintering, they just change from the minor to the dominating trapping sites.

The τ_2-component observed in Z3E, Z3G, and Z3L ceramics may partially arise from remnant effect of misfit vacancy-like defects along GBs, but a major contribution to this component apparently comes from positron trapping in V_{Zr}-based defect complexes situated inside grains (e.g. a V_{Zr}–V_O divacancy or a V_{Zr}–V_O divacancy associated with a RE cation). Unfortunately, statistical accuracy of experimental data does not allow for a reasonable quantitative analysis of this situation, e.g. within the simple trapping model [16].

The CDB results obtained for Z3E, Z3G, and Z3L nanopowders and ceramics were shown in Fig. 1 as DBP ratios to Zr reference plotted as functions of the magnitude of electron momentum p_L. For a comparison, DBPs of the well-annealed coarse-grained pure Gd (99.9%) and Lu (99.9%) were measured and included in the figure, too (dashed and full line, respectively). The most remarkable feature exhibited by the Z3E, Z3G, and Z3L ratios of Fig. 1 is a pronounced peak around $p_L \approx 15 \times 10^{-3} m_0 c$. In the light of the DBP ratios for Gd and Lu shown in the figure, it seems unlikely that this peak in the Z3G and Z3L ratio curves is significantly contributed by Gd and Lu electrons.

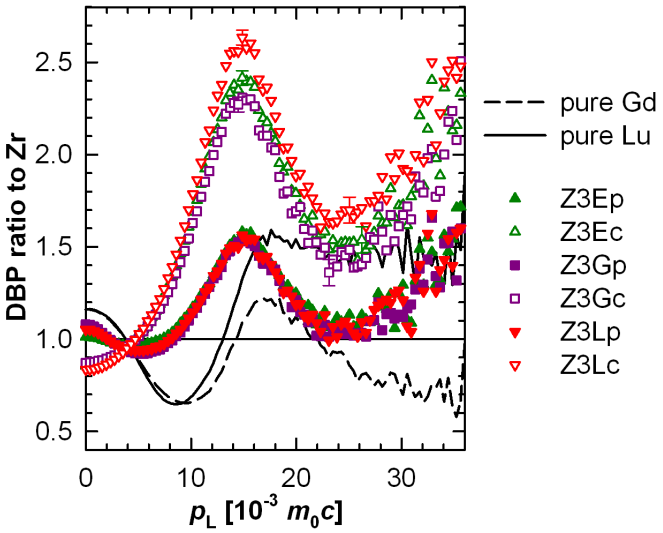

Fig. 1. DBP ratio curves with respect to Zr reference plotted as functions of electron momentum magnitude p_L.

On the other hand, such a peak is known from CDB experiments on numerous metal oxides including zirconia as an effect of positron annihilations with the oxygen $2p$ electrons [12, 13] and this interpretation should be accepted also for Z3G and Z3L. Since the DBP ratios for the three nanopowders were found to be virtually identical to each other in the peak region around $p_L \approx 15 \times 10^{-3} m_0 c$, see full symbols in Fig. 1, the same nature of this peak, i.e. annihilations with the oxygen $2p$ electrons, is very likely plausible also for the Z3E. A smaller peak close to $p_L \approx 0$, found in all the three nanopowders (Fig. 1), undoubtedly arises from p-Ps annihilations. The amplitudes of this peak reasonably correlate with the o-Ps intensities of Table II which provides a further symptom of Ps formation in the Z3E, Z3G, and Z3L nanopowders.

Figure 1 also shows that sintering of nanopowders (open symbols) led to a further substantial increase of the peak at $p_L \approx 15 \times 10^{-3} m_0 c$ and to a disappearance of the p-Ps peak at $p_L \approx 0$. The latter phenomenon is an independent indicator of sintering-induced disappearance of pores in ceramics. The former phenomenon implies a growing relative contribution of annihilation sites surrounded with a greater number of oxygen atoms. The most likely candidates for such trapping sites are V_{Zr}-

-like defects in grain interiors [12] and thus, similarly as in the other zirconia nanosystems [12, 13], the increase of the peak at $p_L \approx 15 \times 10^{-3} m_0 c$, observed in Z3E, Z3G, and Z3L in the present work, should be regarded as a significant marker of sintering-induced grain growth.

4. Summary

The positron lifetime and Doppler broadening techniques were applied for the first time to study zirconia nanopowders doped with RE_2O_3 (RE = Eu, Gd and Lu) and ceramics obtained by sintering the nanopowders. In the pressure-compacted nanopowders, positrons were found to annihilate as trapped in defects associated to grain boundaries: the vacancy-like misfit defects and the triple points. A small fraction of positrons forming positronium in pores between crystallites was also observed and the pore size was estimated as ≈ 1.8 nm. Sintering of nanopowders led to a substantial grain growth accompanied by a disappearance of triple points and pores.

Acknowledgments

The present work was financially supported by the Czech Science Foundation under project P108/11/1396 and by the National Academy of Science of Ukraine within the Complex Programme of Fundamental Research of NAS Ukraine "Fundamental problems of nanostructured systems, nanomaterials and nanotechnologies" (project 89/12-H).

References

[1] *Science and Technology of Zirconia*, Vol. V, Eds. S.P. Badwal, M.J. Bannister, R.H.J. Hannink, Technomic Pub. Co., Lancaster (PN) 1993.

[2] *Sintering*, Eds. R.H.R. Castro, K. van Benthem, Springer-Verlag, Berlin 2013.

[3] I.A. Yashchishyn, A.M. Korduban, V.V. Trachevskiy, T.E. Konstantinova, I.A. Danilenko, G.K. Volkova, I.K. Nosolev, *Funct. Mater.* **17**, 306 (2010).

[4] I. Prochazka, J. Cizek, O. Melikhova, J. Kuriplach, W. Anwand, G. Brauer, T.E. Konstantinova, I.A. Danilenko, I.A. Yashchishyn, *Def. Diff. Forum* **331**, 181 (2012).

[5] T. Konstantinova, I. Danilenko, V. Glazunova, G. Volkova, O. Gorban, *J. Nanopart. Res.* **13**, 4015 (2011).

[6] F. Becvar, J. Cizek, I. Prochazka, J. Janotova, *Nucl. Instrum. Methods. Phys. Res. A* **443**, 372 (2010).

[7] I. Prochazka, I. Novotny, F. Becvar, *Mater. Sci. Forum* **255-257**, 772 (1997).

[8] H. Surbeck, *Helv. Phys. Acta* **50**, 705 (1977).

[9] J. Cizek, M. Vlcek, I. Prochazka, *Nucl. Instrum. Methods Phys. Res. A* **623**, 982 (2010).

[10] M. Eldrup, D. Lightbody, J.N. Sherwood, *Chem. Phys.* **63**, 51 (1981).

[11] K. Ito, H. Nakanishi, Y. Ujihira, *J. Chem. Phys. B* **103**, 4555 (1999).

[12] J. Cizek, O. Melikhova, I. Prochazka, J. Kuriplach, G. Brauer, W. Anwand, T.E. Konstantinova, I.A. Danilenko, *Phys. Rev. B* **81**, 024116 (2010).

[13] I. Prochazka, J. Cizek, O. Melikhova, T.E. Konstantinova, I.A. Danilenko, I.A. Yashchishyn, W. Anwand, G. Bauer, *J. Phys., Conf. Ser.* **443**, 012026 (2013).

[14] K. Ito, Y. Yagi, S. Hirano, M. Miyayama, T. Kudo, A. Kishimoto, Y. Ujihira, *J. Ceram. Soc. Japan* **107**, 123 (1999).

[15] O. Melikhova, J. Cizek, I. Prochazka, T.E. Konstantinova, I.A. Danilenko, *Phys. Proc.* **35**, 134 (2012).

[16] P. Hautojärvi, C. Corbel, in: *Positron Spectroscopy of Solids*, Eds. A. Dupasquier, A.P. Mills, Jr., IOS Press, Amsterdam 1995, p. 491.